Transition Metal Chemistry **29**: 495–504, 2004.

Keto-enolic equilibria of an isatin-schiff base copper(II) complex and its reactivity toward carbohydrate oxidation

Giselle Cerchiaro, Patrícia Lopes Saboya and Ana Maria da Costa Ferreira*
Departamento de Química Fundamental, Instituto de Química, Universidade de São Paulo, P.O. Box 26077, São Paulo, SP 05513-970, Brazil

Daniela Maria Tomazela and Marcos Nogueira Eberlin
Departamento de Química Orgânica, Instituto de Química, Universidade Estadual de Campinas, Campinas, SP 13083-970, Brazil

Received 19 January 2004; accepted 22 January 2004

Abstract

An interesting isatin-Schiff base copper(II) complex, [Cu(*isapn*)]$(ClO_4)_2$ where *isapn* = N,N′-[bis-(3,3′-indolin-2-one)]-1,3-diiminepropane, was prepared and characterized by different techniques, both in the solid state and in solution, and its reactivity toward carbohydrate oxidation was verified. The positive ion electrospray mass spectrum detects the complex as an isotopologue cluster of singly charged intact isatin-copper(I) ions of m/z 395 (for ^{65}Cu) with an isotopic pattern identical to that calculated for $C_{19}H_{16}CuN_4O_2^+$. Tandem mass spectrometry reveals an interesting and structurally diagnostic collision-induced dissociation behavior for this ionized complex, which is dominated by the cleavage of the N—$(CH_2)_3$—N propylene bridge. In aqueous solution, this complex undergoes a peculiar keto-enolic equilibrium, verified at different pH's by spectroscopic methods (u.v.–vis. and e.p.r.), with a corresponding pK_a determined as 9.5. The e.p.r. parameter ratio $g_{\|}/A_{\|}$ for this complex, in frozen MeOH/H_2O (4:1, v/v) solution at 77 K, changes from 188 cm in acidic medium (pH 2.5–3.0) to 118 cm in basic medium (pH 11), indicating a significant structural change from a distorted tetrahedral to a more tetragonal geometry around the copper ion. This compound was shown to catalyze the oxidation of hexoses (glucose, fructose and galactose), in alkaline media, *via* reactive oxygen species, which were detected by using specific enzymes, and by e.p.r. spin trapping. The reaction was monitored at (25.0 ± 0.1) °C by the consumption of oxygen, and showed first-order dependence on catalyst, followed by a saturation effect. First-order kinetics with respect to [OH^-] concentration was also observed, indicating that enolization of the substrate as well as the metal-catalyzed enediol oxidation are the rate-determining steps.

Introduction

Isatin is an endogenous indole with a variety of pharmacological actions, including anticonvulsant, antimicrobial and antiviral activities, inhibition of monoamine oxidase [1], and behavioral effects [2]. Moreover, it has been largely used as a versatile reagent in organic synthesis, to obtain heterocyclic compounds, and as raw material for drugs [3]. Some synthetic oxindole-based compounds have been developed as potent inhibitors of human rhinovirus protease and tyrosine kinase [4], and others were proposed as anticancer, anti-HIV or antimicrobial agents [5]. More recently, the cytotoxicity of isatin and the action of other endogenous oxindoles as antiproliferative and proapoptotic compounds were also reported [6, 7].

Several copper(II) complexes with isatin and its derivatives have been described in the literature [8]. Compounds with quinolylhydrazones derived from isatin had their spectroscopic and magnetic properties investigated [9]. Lately, isatin-thiosemicarbazone copper(II) complexes related to the antiviral drug, methisazone, were prepared electrochemically or by usual condensation methods, being characterized by different spectroscopic techniques [10]. This type of complex was found to cause significant inhibition of human leukaemic cell proliferation [11], presenting the copper atom in a square pyramidal coordination, as determined by crystallographic analyses [12]. Nickel(II) chelates, and some hetero binuclear complexes where metal centers were copper(II), uranium(II), or lanthanum(III), with isatin-Schiff base ligands were also obtained [13], including the precursor *N*,*N*′-bis(indol-2-oxo-3-ylidene)-1,3-diaminopropane copper(II) complex, however its structural properties and reactivity have not yet been investigated.

Isatin exhibits an interesting keto-enolic equilibrium that can influence its coordination properties, giving rise to cationic or neutral complexes with varied structure

* Author for correspondence

and reactivity [14]. Similar keto-enolic species are also involved in the oxidation of carbohydrates, a process catalyzed by copper ions, where enediol radicals are formed simultaneously to the reduction of the metal center, and reactive oxygen species are reported as intermediates [15]. Ligands derived from isatin could then modulate the reactivity of the metal coordinating center, contributing to the catalysis in oxidative processes.

Carbohydrate oxidation has been implicated in many diseases, such as diabetes mellitus, cataracts, atherosclerosis, Alzheimers disease and aging in general, mainly by a so-called glycoxidation process [16] involving non-enzymatic glycation of proteins, Maillard reaction, and further oxidation of intermediate products, deserving extensive studies in the last decades [17, 18]. In all these reactions, copper ions play a fundamental role [19].

Aiming to shed light on the mechanism of oxidative processes initiated by copper(II)–carbohydrate interactions, we initiated the present study by choosing copper(II) complexes that exhibited a keto-enolic equilibrium similar to that showed by coordinated sugars. In a previous study, enediol-type ligands coordinated to copper ions have been shown to be crucial for the oxidation of gluconate and glucuronate [20]. Herein, an isatin-Schiff base copper(II) complex was isolated and its different tautomeric forms were monitored in aqueous solution, characterized mainly by their spectroscopic properties. Subsequently, its catalytic activity toward carbohydrate oxidation in alkaline medium was verified.

Experimental

Materials and methods

Carbohydrate substrates used in the kinetic studies: D(+)Glucose (99%), and D(−)Fructose (99%) were obtained from Merck, and D(+)Galactose (99%) from Sigma Chemical Co. Isatin (98%), 1,3-diaminopropane, and catalase (from bovine liver) were purchased from Aldrich. Cu,Zn SOD from bovine erythrocytes was from Sigma Chemical Co. DMPO (2,2′-dimethyl-pyrroline-*N*-oxide, from Aldrich) was previously purified as recommended [21]. DBNBS (3,5-dibromo-4-nitrosobenzenesulfonate) was prepared from 3,5-dibromosulphanilic acid and glacial acetic acid, by a procedure previously described [22]. All other reagents were P.A. grade, from different sources. Deionized water from a Barnstead D 4700 apparatus was used in the preparation of all solutions.

Elemental analyses were performed at the *Central Analítica* of our Institution, using a Perkin-Elmer 2400 CNH Elemental Analyzer. Copper analyses were performed in a SPECTRO ICP-AES (Induced Coupled Plasma) SpectroFlame. Samples were initially treated with concentrated HNO_3 (P.A.), followed by addition of 30% H_2O_2 (5 cm^3 each), and heated for 1 h (at 80–90 °C). The mass spectrometric measurements were performed using a high resolution hydrid quadrupole (Q) and orthogonal time-of-flight (Tof) mass spectrometer (QqTof from Micromass, UK) operating in the positive ion electrospray ionization mode. The nebulizer temperature was 200 °C, and the cone voltage was 40 V. The tandem mass spectrum (MS/MS) was acquired using the product ion scan mode *via* Q1 mass-selection of the singly charged complex, its collision-induced dissociation (CID) with N_2 at 15 eV energy in q2, and high-resolution orthogonal T of mass analysis of the CID ionic fragments. I.r. spectra of the complexes obtained were recorded in a BOMEM 3.0 instrument, in the 4000–400 cm^{-1} range, using KBr pellets. E.p.r. spectra were recorded on a Bruker EMX spectrometer, operating at the X-band frequency, 20 mW potency and 100 kHz field modulation, using standard Wilmad quartz tubes. DPPH (α,α'-diphenyl-β-picrylhydrazyl) was used as the magnetic field calibrant ($g = 2.0036$), with samples in frozen $MeOH/H_2O$ (4:1, v/v) solution, at 77 K. Usual conditions used in these measurements were 15 G modulation amplitude, and 2.00×10^4 receiver gain. The u.v.–vis. spectra were registered in an Olis modernized-Aminco DW 2000 or a Beckman DU-70 spectrophotometer, in standard 10 mm quartz cells. The pH value of solutions during e.p.r. and u.v.–vis. experiments was adjusted using appropriate amounts of 0.1 mol dm^{-3} HCl or NaOH solutions, and monitored on a Digimed DMPH-2 instrument, coupled to a combined pH electrode, from *Ingold or Radiometer*. The pH meter was calibrated with appropriate buffer solutions, at (25 ± 1) °C. Conductivity measurements with 1.0 mmol dm^{-3} aqueous solution of the complexes studied were carried out on a Digimed DM-31 instrument, using a 10.0 mmol dm^{-3} KCl solution as standard (specific conductivity = 1412.0 $\mu S\ cm^{-1}$, at 25.0 °C) [23].

Syntheses of the complexes

Two copper(II) complexes with Schiff base ligands were prepared as perchlorate salts.

Caution
Although the prepared species were shown to be very stable, perchlorate salts of metal complexes with organic ligands are potentially explosive, and should be very carefully handled, only in small amounts.

[Cu(isapn)](ClO$_4$)$_2$
The isatin-diimine copper(II) complex *(1)*, *Cu*(*isapn*)-*(*ClO_4*)$_2$*, was synthesized by condensation of 1,3-diaminopropane (*pn*) with isatin (*isa*) dissolved in EtOH solution, followed by coordination to copper(II) ions, added as perchorate the salt, according to a standard literature procedure, with suitable modifications [24]. During the reaction, an apparent pH of ∼5.5 was maintained. The isolated blue crystals were recrystallized from ethanoldiethyl ether solution. Yield: 85%. (Found: C, 38.5; H, 2.9; N, 9.5; Cu, 10.5. $C_{19}H_{16}N_4O_2$-

$Cu(ClO_4)_2$ calcd.: C, 38.4; H, 2.75; N, 9.4; Cu, 10.7%.) $\Lambda_M = 81.5$ S cm^2 mol^{-1} in H_2O, and 57.6 S cm^2 mol^{-1} in MeOH (both at 25 °C). FT-IR (cm^{-1}, KBr): 3447 (m, NH or OH) and 3334 (m, NH); 3102–2774 (w, $C_{sp2}H$ and C═C); 1734 (s, CO amide); 1665 (s, O—H); 1616 (s, N—H); 1591 (s, C═N); 1459 (m, C—O); 1102 and 625 (s, ClO_4 no coordinated). MS (ESI+): *m*/*z* found: 395.02 (calcd.: 395.07, for $C_{19}H_{16}N_4O_2Cu$).

[Cu(quipn)](ClO$_4$)$_2$

This compound *(2)* was prepared by an analogous procedure, where *quipn* = Schiff base derived from 2-quinolynecarboxaldehyde and 1,3-diaminopropane, for the purpose of comparative reactivity. Yield: 65%. (Found: C, 44.7; H, 3.3; N, 9.1. $C_{23}H_{20}N_4Cu(ClO_4)_2$ calcd.: C, 44.9; H, 3.3; N, 9.1%. $\Lambda_M = 208$ S cm^2 mol^{-1} in H_2O, and 130.0 S cm^2 mol^{-1} in methanol (both at 25 °C). FT-IR (cm^{-1}, KBr): 3069–2945 (w, $C_{sp2}H$ and C═C); 1589 (s, C═N); 1097 and 624 (s, ClO_4 no coordinated). MS (ESI+): *m*/*z* found: 415.09 (calcd.: 415.98, for $C_{23}H_{20}N_4Cu$).

Kinetic measurements

Kinetic measurements were carried out in a GILSON oxygraph apparatus (Medical Electronics Inc. USA), monitoring the oxygen consumption during the catalytic oxidation of carbohydrates. A Clark Pt electrode was used as O_2 probe, with internal reference Ag/AgCl, and YSI membrane (from Yellow Spring Instruments Co.), with saturated KCl solution between the electrode and the membrane. A standard cell was utilized in these experiments, with a total vol of 1.8 cm^3, closed by a capillary cap with no oxygen exchange through the atmosphere, and wrapped in a thermostat bath at (25.0 ± 0.1) °C. Sodium dithionite was used to calibrate the oxygraph. The solubility of O_2 was taken as 244 μmol dm^{-3} O_2 dissolved in pure H_2O, at 25.0 °C [25]. The experiments were performed in basic medium, using 250 mmol dm^{-3} carbonate buffer (Na_2CO_3/NaOH), pH (12.0 ± 0.2), previously treated with Chelex resin to eliminate any metal traces. The stock solutions of the complexes were 1.0 mmol dm^{-3} in carbonate buffer, and adequate volumes were added to the oxygraph cell, to make the suitable final concentration of the catalyst in the 10^{-6}–10^{-4} mol dm^{-3} range. The stock solutions of carbohydrates were usually 10.0 mmol dm^{-3}, and were afterwards diluted to the final 1.00 mmol dm^{-3} concentration. All the kinetic measurements were recorded at least in triplicate.

Results and discussion

The isatin-Schiff base copper(II) complex, [Cu(*isapn*)]$(ClO_4)_2$ (structure *1A* in Scheme 1), was isolated from ethanol solution, and characterized by elemental analysis, conductivity measurements, u.v.–vis. i.r. and e.p.r. spectroscopy, and additionally by positive ion electrospray mass, and tandem mass spectrometry. In the literature, the neutral enol-form of this complex has been poorly described [13]. An analogous compound, [Cu(*quipn*)]$(ClO_4)_2$ (structure *(2)*, Scheme 1), was also obtained and characterized, for the purpose of comparative catalytic studies.

I.r. spectra

The recorded spectra of [Cu(*isapn*)]$(ClO_4)_2$, in KBr pellets, showed the expected characteristic bands of a

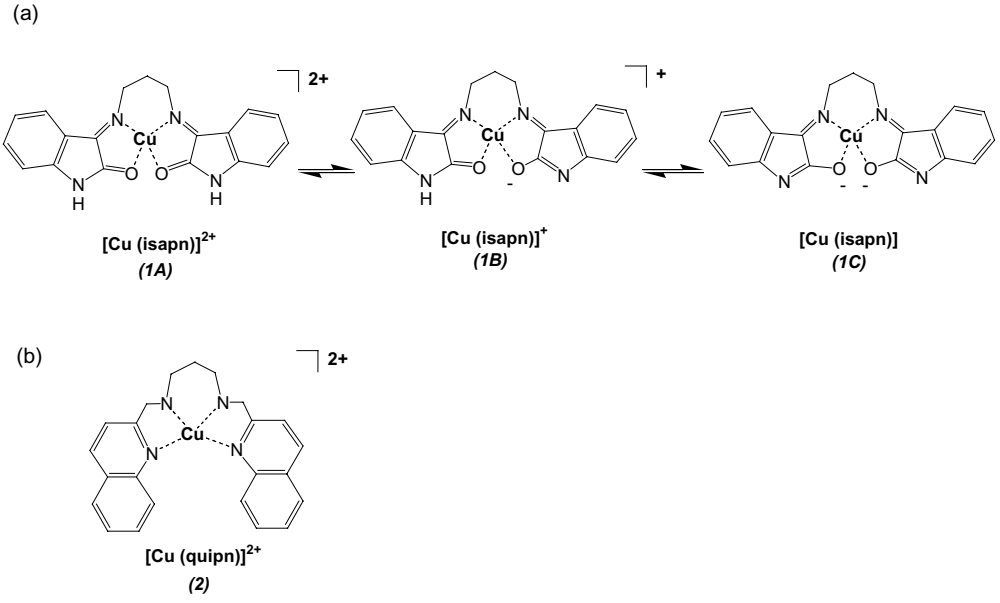

Scheme 1. (a) Equilibria involving different forms of the complex [Cu(*isapn*)]$^{2+}$ *(1)*, in the range of pH 2.5–11.0; (b) Structure of complex [Cu(*quipn*)]$(ClO_4)_2$ *(2)*.

diimine compound, as indicated in the Experimental section. The bands observed at 3447 and 3334 cm^{-1} were assigned to ν(N—H), although the first one could be also attributed to ν(OH), if the corresponding enol form is present as an impurity. In this case, the band at 1665 cm^{-1} was probably due to δ(OH). The bands at *ca.* 3102–2774 cm^{-1} can be attributed to $\nu(C^2_{sp}—H)$ and $\nu(C^3_{sp}—H)$, while the corresponding bending modes were verified in the 990–750 cm^{-1} range. The characteristic ν(C=N) frequency was found at 1591 cm^{-1}. The additional strong band observed at 1734 cm^{-1} is characteristic of ν(C=O) amide, and the band at 1616 cm^{-1} of δ(N—H). These data were particularly important in order to recognize that the complex, as obtained in the solid state, is mostly in the keto-form, and confirmed previous data by elemental analyses. Additional bands observed at 1102 and 625 cm^{-1} are characteristic of non-coordinated perchlorate ions. Therefore, those data are consistent with the proposed formula $C_{19}H_{16}N_4O_2Cu(ClO_4)_2$ and structure *1A* (see Scheme 1), being corroborated by results from other techniques.

Analogous i.r. spectra were registered for the complex *(2)* [Cu(*quipn*)]$(ClO_4)_2$. In this case, the strong characteristic ν(C=N) frequency was found at 1589 cm^{-1}, and no ν(C=O) bands at *ca.* 1730 or δ(N—H) the band at ~1600 cm^{-1} were detected. The bands at *ca.* 3069–2945 cm^{-1} were attributed to $\nu(C_{sp2}—H)$ and $\nu(C_{sp3}—H)$. As well, the expected bands of non-coordinated perchlorate ions were observed at 1097 and 624 cm^{-1}.

For both complexes, additional characterization by mass spectrometry and e.p.r. spectroscopy was achieved, in order to obtain complementary structural information.

Conductivity measurements

The conductivity measurements of the studied complex *(1)* in deionized water or methanol, at 298 K, as indicated in the experimental section, are consistent with a 1:1 electrolyte [23]. The pH measured in a 1.00 mmol dm^{-3} aqueous solution of this complex was 5.8, indicative of an equilibrium very dependent on protonation. Here, a tautomer form different from that isolated in the solid state is predominant, and is ascribed probably to structure *1B* in Scheme 1. The enolic equilibrium of this type, also observed with the free indole, is very dependent on the pH of the solution.

For complex *(2)*, there is no possibility of a tautomer equilibrium, and the corresponding results indicated a 2:1 electrolyte, both in water and in ethanol, corroborating other data.

Mass spectroscopy studies

Although electrospray mass (and tandem mass) spectrometry has been mainly and most successfully applied to the analysis of biomolecules [26], it has being increasingly used as a powerful structural characterization technique for organometallic and coordination compounds [27], transient intermediates [28], as well as to study intrinsic coordination catalysis [29]. Figure 1A shows the positive ion electrospray mass spectrum of the isatin-Schiff base copper(II) complex *(1)* acquired from a 1:1 acetonitrile:water solution. As copper displays two abundant isotopes [^{63}Cu (69.2%) and ^{65}Cu (30.8%)] in a 1:0.44 abundance ratio, the intact cationic complex is detected as an isotopomeric cluster of singly charged ions of *m/z* 395 (for ^{63}Cu) with the second most abundant ion of *m/z* 397 (mostly due to ^{65}Cu), and with an isotopic pattern that matches perfectly that calculated for $C_{19}H_{16}CuN_4O_2^+$ (Figure 1B). Note that in the course of ESI the doubly charged $C_{19}H_{16}Cu(II)N_4O_2^{+2}$ complex was reduced to its singly charged copper(I) form $C_{19}H_{16}Cu(I)N_4O_2^+$, a common charge-reducing process for gaseous highly charged coordination cations under ESI conditions [28]. Mass-selection of the singly charged cluster of $C_{19}H_{16}Cu(I)$-$N_4O_2^+$ ions and its CID with nitrogen at 15 eV energy in a tandem mass (MS/MS) spectrometric experiment reveals a structurally diagnostic and interesting dissociation behavior, as depicted in Scheme 2. Dissociation occurs mainly at the propylene N—$(CH_2)_3$N 'bridge': a

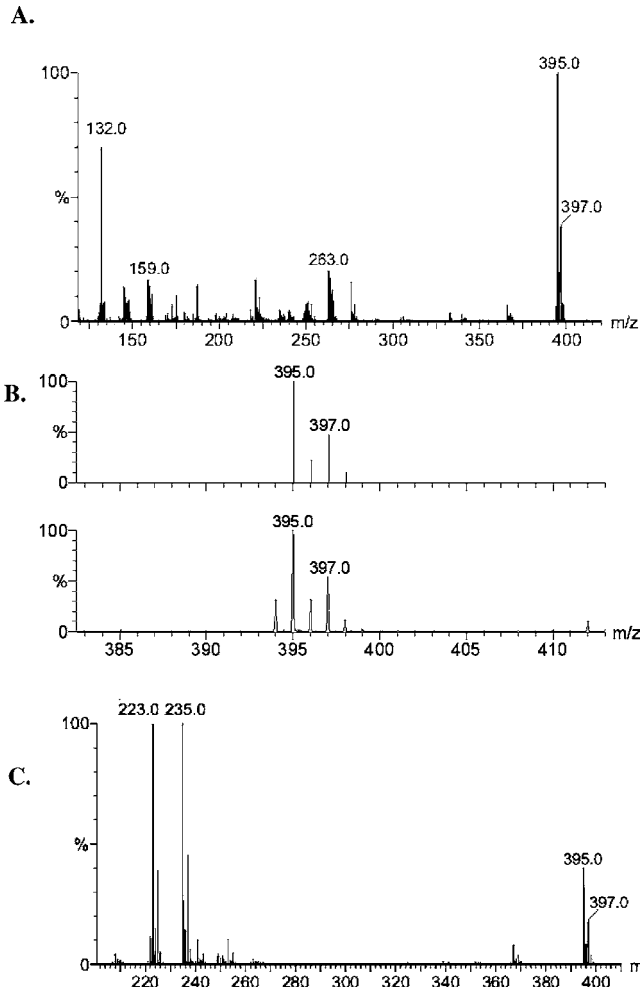

Fig. 1. (A) Positive ion electrospray mass spectrum for a 1:1 MeCN:H_2O solution of [Cu(*isapn*)]$(ClO_4)_2$. (B) Theoretical and observed isotopic pattern for the intact $[Cu(isapn)]^+$ cations. (C) Product ion mass spectrum for CID of the isotopologue cluster of $[Cu(isapn)]^+$ ions of at *m/z* 395.

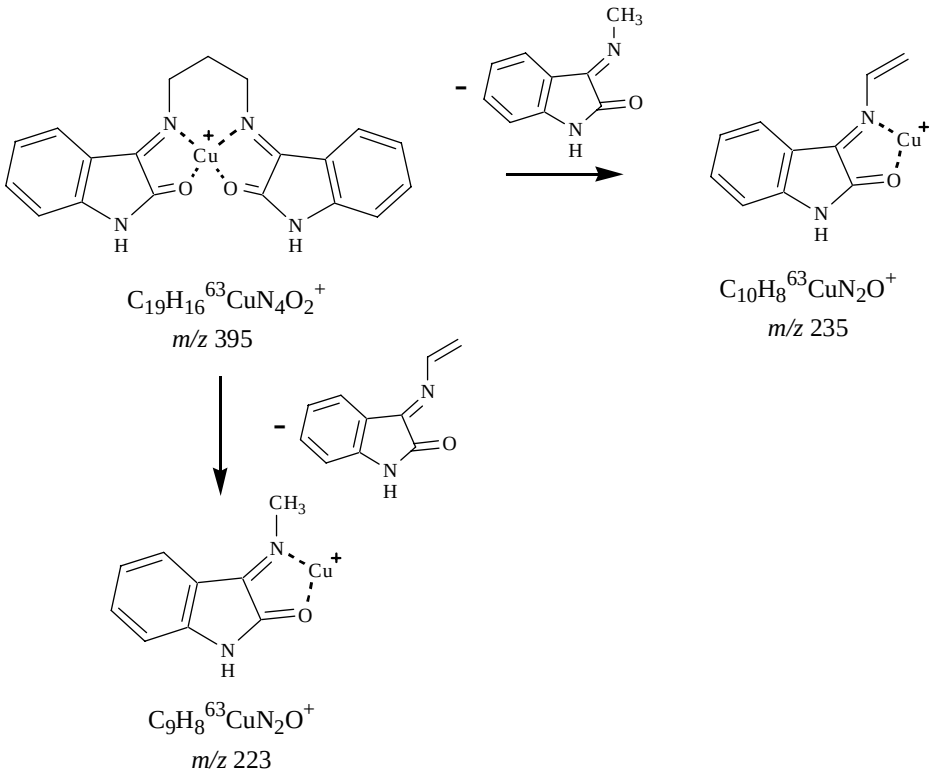

Scheme 2. Fragmentation pattern of the complex $[Cu(isapn)]^{2+}$ observed by CID.

[1,3-H] shift is accompanied by *N*—C1 bond breaking that forms both a *N*-methyl and a *N*-vinyl isatin derivative. Thus, both neutral isatin fragments compete for Cu^+ to form the two main and nearly equal abundant $^{63}Cu/^{65}Cu$-containing fragment ions of *m/z* 223 (225) and 235 (237) with their characteristic Cu-isotopic patterns, see Figure 1C.

Therefore, these results complemented previous characterization of complex *(1)* as a cationic species, with the corresponding keto-form of the coordinated isatin-Schiff base ligand.

Analogous results for complex *(2)* were obtained (data not shown). In this case, fragments of singly charged ions of at *m/z* 415 (for ^{63}Cu), with the second most abundant ion of *m/z* 417 (mostly due to ^{65}Cu), and with an isotopic pattern that matches perfectly that calculated for $C_{23}H_{20}CuN_4^+$ were observed.

Electronic spectra

The electronic spectrum of $[Cu(isapn)]^{2+}$ was recorded in aqueous solution, and the corresponding maximum wavelengths were observed at 242 nm ($\varepsilon = 5.1 \times 10^3$ mol^{-1} dm^3 cm^{-1}), corresponding to internal ligand transitions ($n \rightarrow \pi$, or $n \rightarrow \pi^*$); 303 nm ($\varepsilon = 2.7 \times 10^3$ mol^{-1} dm^3 cm^{-1}), and 402 nm, with a shoulder at 434 nm ($\varepsilon = 1.6 \times 10^3$ mol^{-1} dm^3 cm^{-1}), attributed to LMCT transitions ($\pi \rightarrow d\pi$). In DMF solution, where the complex is more soluble, the characteristic d–d band appears at 688 nm ($\varepsilon = 151$ mol^{-1} dm^3 cm^{-1}). In previous related work [30], some metal complexes with the isatin-3-hexamethyleneiminylthiosemicarbazone ligand were reported, showing very similar data, typically with intra-ligand bands at 261, 289 and 361 nm, and LMCT band at 400 and 448 nm, and the $d \rightarrow d$ band at 601 nm.

Changes in the electronic spectrum of the complex studied at different pHs were monitored by addition of HCl, or NaOH (0.1 mol dm^{-3}). A new band was detected at 354 nm, with concomitant shift of the maximum absorption corresponding to LMCT transitions, at 402 nm, in alkaline medium, as shown in Figure 2A. These data corroborated the previous conductivity measurements, since the enolic form is favored at higher pH, and is expected to show more intense c.t. bands, at higher energy. A plot of pH *versus* $\log [(A - A_{min})/(A_{max} - A)]$, where A = absorbance of the new band at $\lambda = 354$ nm, shown in Figure 2B, permitted the calculation of a pK_a of 9.5, consistent with the formation of structure *1C* in Scheme 1.

For complex *(2)* $[Cu(quipn)]^{2+}$, internal ligand transitions were observed at 206 nm ($\varepsilon = 5.0 \times 10^4$ mol^{-1} dm^3 cm^{-1}), and 251 nm ($\varepsilon = 4.9 \times 10^4$ mol^{-1} dm^3 cm^{-1}). The characteristic d–d band appears at 665 nm ($\varepsilon = 135$ mol^{-1} dm^3 cm^{-1}), and an intense LMCT ($\pi \rightarrow d\pi$) is observed at 336 nm ($\varepsilon = 1.1 \times 10^4$ mol^{-1} dm^3 cm^{-1}).

E.p.r. studies

E.p.r. spectra of the obtained complex *(1)* $[Cu(isapn)]^{2+}$ in frozen methanol:water solutions showed a characteristic profile of an axial environment around the cop-

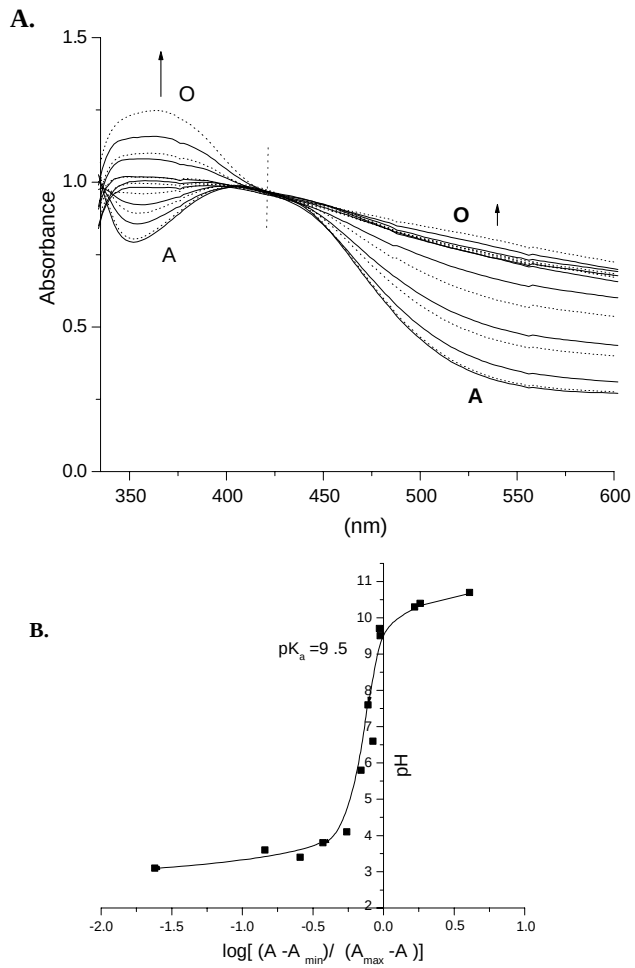

Fig. 2. (A) u.v.–vis. spectra of the complex $[Cu(isapn)]^{2+}$ 0.5 mmol dm^{-3}, at different pHs (A–O): (a) 2.7, (b) 3.1, (c) 3.4, (d) 3.6, (e) 3.8, (f) 4.1, (g) 5.8, (h) 6.6, (i) 7.6, (j) 9.5, (k) 9.7, (l) 10.3, (m) 10.4, (n) 10.7, (o) 11.3. (B) Plot of pH *versus* log $[(A - A_{min})/(A_{max} - A)]$, at $\lambda = 354$ nm.

per(II) center, with a $g_{\parallel} > g_{\perp}$. Significant variations in these parameters were verified with increasing pH, in the range 2.5–11.0, as shown in Figure 3. The ratio $g_{\parallel}/A_{\parallel}$ changes from 188 cm in acidic pH to 118 cm in alkaline pH (Table 1), indicating a substantial geometry change from a distorted tetrahedron to a more square planar or tetragonal structure around the copper(II) ion [31]. These data supplemented the previously discussed spectral variations in the u.v.–vis. range, confirming the coexistence of three different species of the complex in aqueous solution, with predominance of one of them depending on the pH of the solution.

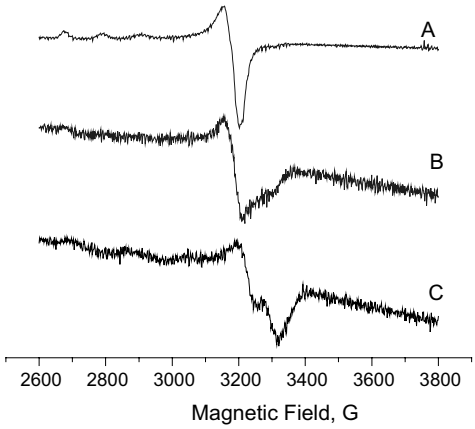

Fig. 3. E.p.r. spectra of the complex $[Cu(isapn)]^{2+}$, in frozen EtOH/H_2O solution, at different pHs: (A) 3.0, (B) 5.6, (C) 11.0.

The analogous spectra for complex *(2)* indicated e.p.r. parameters consistent with those expected for the copper ion in a tetragonal structure (also shown in Table 1), and very close to those for the enol-form of complex *(1)*.

Kinetic studies

According to the conductivity measurements and spectroscopic data, an equilibrium involving the keto- and enol-form of the complex $[Cu(isapn)]^{2+}$ was detected in aqueous solution (Scheme 1). Based on the similarity of these species with the intermediary compounds detected in monosaccharide oxidations and in Maillard reactions [16], the catalytic activity of this copper complex was tested for the oxidation of hexoses.

Kinetic experiments, monitoring the oxygen consumption in the oxidation of fructose, glucose or galactose, showed that the studied complex *(1)* $[Cu(isapn)]^{2+}$ catalyzes these reactions. Experimental curves of O_2 consumed *versus* time, at pH 12.0, indicated that fructose was the most reactive substrate. As shown in Figure 4, the base-catalyzed enolization of the substrate [32] (curve B) is much slower than the metal-catalyzed step (curves D–I, for [catalyst] ≥ 6 μmol dm^{-3}).

A first-order dependence of the initial reaction rate with the catalyst concentration was observed for all substrates, at very low concentrations, followed by a saturation effect at [catalyst] $> 2.0 \times 10^{-5}$ mol dm^{-3} in the case of fructose and glucose, or $>1.0 \times 10^{-4}$ mol dm^{-3} for galactose (see Figure 5A). Based on these data the observed initial rate constant

Table 1. E.p.r. parameters for complexes $[Cu(isapn)]^{2+}$ *(1)* and $[Cu(quipn)]^{2+}$ *(2)* in frozen MeOH/H_2O (4:1, v/v) solution, at 77 K

Complex	PH	E.p.r. parameters			
		$g_{\perp}$	$g_{\parallel}$	$A_{\parallel}$, 10^{-4} cm^{-1}	$g_{\parallel}/A_{\parallel}$, cm
$[Cu(isapn)]^{2+}$	3.0	2.094	2.340	124	188
	5.6	2.091	2.301	126	183
	11.0	2.065	2.240	189	118
$[Cu(quipn)]^{2+}$	–	2.060	2.409	192	125

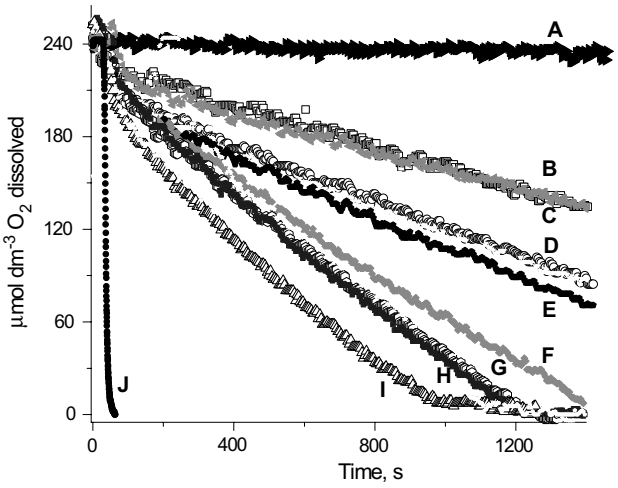

Fig. 4. Kinetic curves of oxygen consumption *versus* time during fructose oxidation catalyzed by $[Cu(isapn)]^{2+}$, at $T = (25.0 \pm 0.1)$ °C, and pH 12.0, in carbonate buffer (250 mmol dm^{-3}). [Fructose] = 1.00 mmol dm^{-3}. (A) No substrate, $[Cu(isapn)]^{2+} = 1.11 \times 10^{-4}$ mol dm^{-3}; (B) no catalyst; (C) $[Cu(isapn)]^{2+} = 2.88 \times 10^{-6}$ mol dm^{-3}; (D) 5.56×10^{-6} mol dm^{-3}; (E) 8.33×10^{-6} mol dm^{-3}; (F) 2.88×10^{-5} mol dm^{-3}; (G) 5.56×10^{-5} mol dm^{-3}; (H) 8.33×10^{-5} mol dm^{-3}; (I) 1.11×10^{-4} mol dm^{-3}; (J) Calibration curve (after addition of sodium dithionite).

was calculated as $(124 \pm 4) \times 10^{-3}$ s^{-1} for the fructose substrate. For glucose and galactose, analogous kinetic studies were made, and the determined k_{obs} values were $(16.5 \pm 0.5) \times 10^{-3}$ s^{-1} $(5.2 \pm 0.1) \times 10^{-3}$ s^{-1}, respectively. These results are conflicting with old results in the literature, when only very high concentrations of carbohydrates were used (at least 2.0×10^{-4} mol dm^{-3}), and zero-order dependence on copper concentration was verified [32].

However, our data also showed an additional metal-non-catalyzed step, attributed only to the base-catalyzed enolization of the substrate, with $V_o = (0.73 \pm 0.02) \times 10^{-6}$ mol dm^{-3} s^{-1} for fructose. This value is actually consistent with earlier literature data ($k_s = 5.65 \times 10^{-5}$ mol l^{-1} min^{-1} $= 0.94 \times 10^{-6}$ mol dm^{-3} s^{-1}) for the enolization step independent of copper concentration, in the D-fructose oxidation [32].

The higher reactivity of fructose, when compared to the other carbohydrates, can be ascribed to the structure of the enediol intermediate formed. The reaction in this case probably occurs at the secondary carbon, leading to a diketone product, while in the others a ketoaldehyde derivative is formed [33]. In the literature, an enediol/carbonyl ratio of 2.3 was reported for D-fructose, in neutral aqueous solution at 30 °C, based on FT-IR spectroscopy studies [34].

Considering that the base-catalyzed enolization is the rate-determining step for carbohydrate oxidation [32], and that the studied catalyst shows different structures with increasing pH, the influence of [OH$^-$] was also verified. A first order dependence was observed, as shown in Figure 6, with $Vi = k_2 + k_3$ [OH$^-$], where $k_2 = (1.3 \pm 0.1) \times 10^{-8}$ mol dm^{-3} s^{-1}, and $k_3 = (4.6 \pm 0.1) \times 10^{-6}$ s^{-1}.

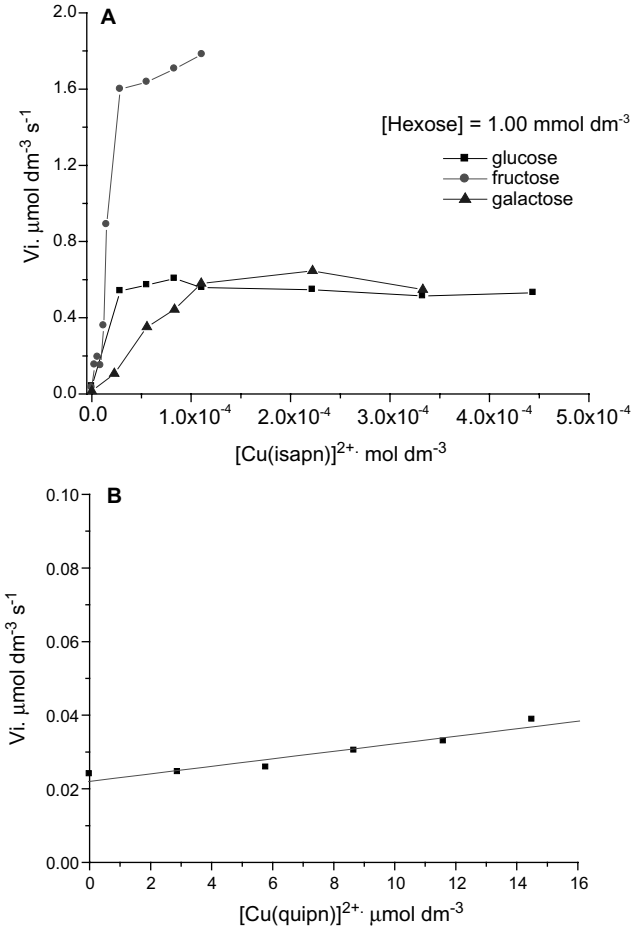

Fig. 5. Dependence of the initial rate of catalyzed carbohydrate oxidation with [catalyst] concentration. Reaction at $T = (25.0 \pm 0.1)$ °C, and pH 12.0, in carbonate buffer (250 mmol dm^{-3}). (A) [CuL] = $[Cu(isapn)]^{2+}$; [Hexose] = 1.00 mmol dm^{-3}. (B) [CuL] = $[Cu(quipn)]^{2+}$; [Fructose] = 1.10 mmol dm^{-3}.

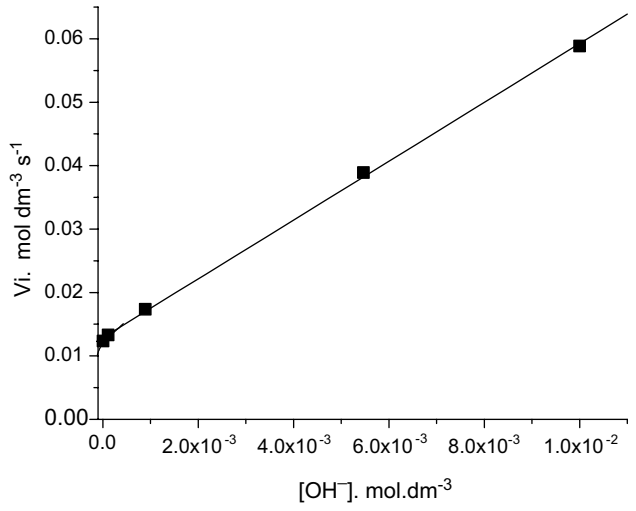

Fig. 6. Initial rate of oxygen consumption *versus* [OH$^-$] during fructose oxidation catalyzed by $[Cu(isapn)]^{2+}$, at $T = (25.0 \pm 0.1)$ °C. $[Cu(isapn)]^{2+} = 0.100$ mmol dm^{-3}, [Fructose] = 1.00 mmol dm^{-3}.

Furthermore, a similar copper complex with no tautomeric forms, complex ***(2)*** $[Cu(quipn)](ClO_4)_2$, was

verified as being almost unreactive as a catalyst on fructose oxidation, at the 10^{-6} mol dm^{-3} concentration range, as shown in Figure 5B, exhibiting an initial rate constant of 1.52×10^{-4} s^{-1}. As shown in Table 1, this complex exhibited very like e.p.r. hyperfine parameters to the enol-form of the active complex *(1)*, indicating the same square planar or tetragonal structure around the copper(II) ion.

Therefore, the kinetic data indicated that both processes, the base-catalyzed substrate enolization and the metal-catalyzed enediol oxidation, are rate-determining steps in the range of concentrations used. These results also indicate that the enediol form of the complex (structure *1C* in Scheme 1) is the main catalytically active species.

Detection of intermediates

In order to detect intermediary species in these catalyzed oxidations of carbohydrates, e.p.r. spin trapping experiments were performed using DMPO and DBNBS as scavengers for free radicals. The presence of DMPO resulted in formation of DMPO-OH adduct, although obtained in very low concentration, with $A_N = A_H = 14.9$ G, at pH 12.0 (phosphate buffer 25 mmol dm^{-3}) for fructose, galactose and glucose (Figure 6). With fructose, no evidence for other adducts were detected. In the case of glucose and galactose, a further adduct, probably due to carbon centered radicals, with $A_N = 15.7$, and $A_H = 18.8$ G, was also observed. This adduct can be ascribed to the formation of the $CO_2^{\bullet -}$ radical anion, whose reported hyperfine constants are $A_N = 15.8$, and $A_H = 18.8$ G [35]. These results are expected since glucose and galactose can form the corresponding aldonates (gluconate, and galactonate), in addition to formate [33]. Similar intermediates of reaction have been previously detected in the copper-catalyzed oxidation of gluconate and glucuronate ions, generating carbonate anions as final product [19]. In the case of fructose, the formation of diketone products is presumably favored, without generation of formate and $CO_2^{\bullet -}$ radical anion (Figure 7).

Further experiments, for identification of carbon centered radicals derived from carbohydrates, using DBNBS as spin trap were carried out. However, DBNBS was shown to be oxidized at the high pH of reaction, possibly to a nitrosyl radical, showing a characteristic spectrum with three lines ($A_N = 9$ G, not shown) already observed in other studies [36]. At lower pH (8–10) the observed carbohydrate oxidation was very slow, and radical formation was undetectable with all the substrates, in similar e.p.r. experiments using both spin traps.

Superoxide radicals were identified by the addition of Cu-Zn and SOD at different times of reaction, causing a temporary suppression of the fructose oxidation, as shown in Figure 8A. Analogous experiments permitted verification of the formation of hydrogen peroxide (Figure 8B). By adding catalase during the kinetic run,

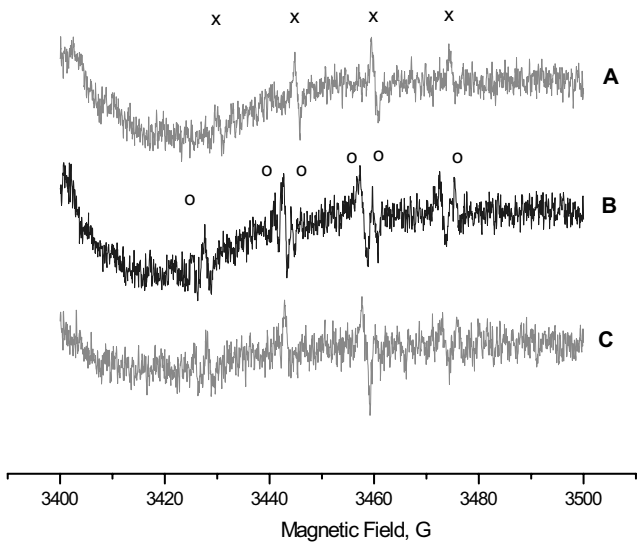

Fig. 7. Spin trapping e.p.r. experiments, using DMPO (50 mmol dm^{-3}) as spin scavenger. Spectra recorded after 5 min of reaction, at 25 °C and pH = 12.0, in phosphate buffer (25 mmol dm^{-3}). [Cu(*isapn*)]$^{2+}$ = 100 μmol dm^{-3}. [Substrate] = 1.00 mmol dm^{-3}: (A) Fructose; (B) Galactose; (C) Glucose. Conditions: modulation amplitude = 1G; Gain = 2.00×10^5; 8 scans.

liberation of oxygen was observed, corresponding to 12 μmol dm^{-3} after 290 s, and 20 μmol dm^{-3} of H_2O_2 after 425 s. Both intermediates, the superoxide radical and hydrogen peroxide, react subsequently with the copper species being dismutated or decomposed.

Concluding remarks

The obtained data revealed different forms of the complex [Cu(*isapn*)]$^{2+}$ in aqueous solution, although only its keto-form has been isolated and characterized in the solid state. Spectroscopic data allowed the characterization of each form, corroborated by conductivity measurements and by positive ion electrospray mass, and tandem mass spectrometry. The enolform was found to predominate in alkaline medium, and is probably the most active species in the catalysis of carbohydrate oxidation, verified at pH > 10. Analogous kinetic data using another Schiff base-copper(II) complex, [Cu(*quipn*)]$(ClO_4)_2$, with a very similar environment around the copper center, as attested by e.p.r. parameters, but lacking tautomer forms, showed negligible catalytic activity. Oxygen consumption curves at (25.0 ± 0.1) °C indicated decreasing rate constants in the order: fructose ≫ glucose > galactose. The obtained data are consistent with a mechanism involving base-catalyzed substrate enolization and metal-catalyzed enediol oxidation as rate-determining steps, although further kinetic experiments are required for complete determination of the rate law.

Spin trapping e.p.r. experiments revealed that the oxidation process is probably mediated by the hydroxyl radical, mostly bound copper-hydroxyl species,

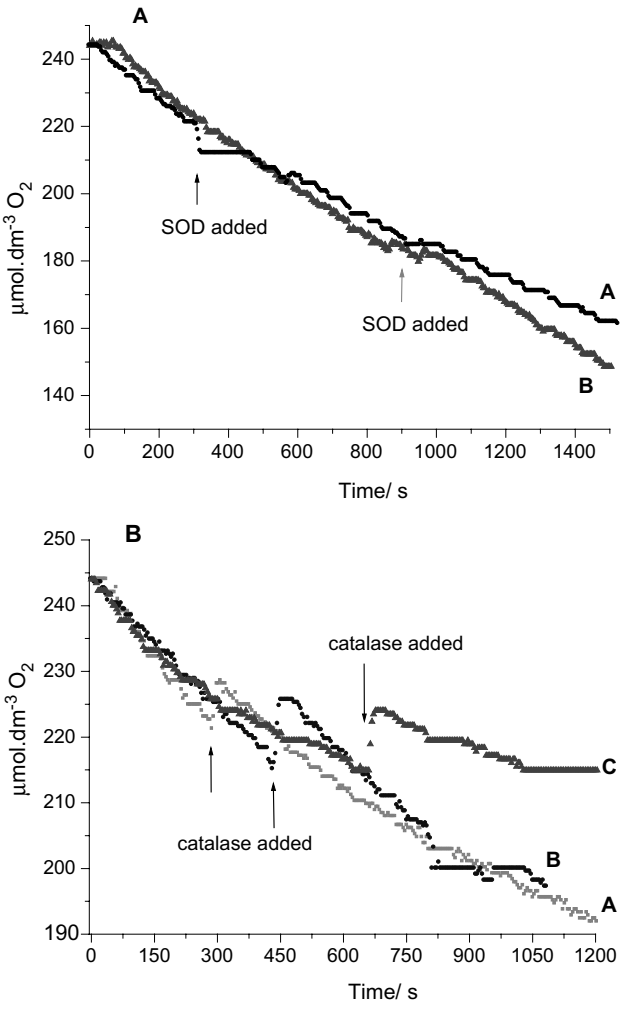

Fig. 8. (A) Addition of Cu, Zn-SOD (15000 u.) during kinetic run of fructose (1.00 mmol dm^{-3}) oxidation catalyzed by $[Cu(isapn)]^{2+}$ (0.10 mmol dm^{-3}), at $T = (25.0 \pm 0.1)$ °C and pH 12.0, adjusted with NaOH solution. Addition of Cu,Zn-SOD after 300 s (A), and 900 s (B) of reaction. (B) Addition of catalase (18800 u.) during kinetic run of fructose (1.00 mmol dm^{-3}) oxidation, catalyzed by $[Cu(isapn)]^{2+}$ (0.10 mmol dm^{-3}), at $T = (25.0 \pm 0.1)$ °C, and pH 12.0, adjusted with NaOH solution. Addition of catalase after 290 s (A), 425 s (B), and 650 s (C) of reaction.

$[LCu^{II}(\bullet OH)]$, instead of 'free' radicals as already proved in other systems [37], and with additional formation of $CO_2^{\bullet -}$ radical anion in the case of glucose and galactose, as intermediary species. Inhibition of the reaction by addition of Cu,Zn SOD indicated also the fundamental participation of superoxide anion, in propagation steps. Since this radical anion is a key intermediate in oxidation steps during glycoxidation [19], the studied complex can probably also be reactive toward Amadori rearrangement products, and glycated proteins.

Acknowledgements

This work was supported by the Brazilian agencies CNPq and FAPESP (grants 01/09127-6 and 00/11176-2). The authors are also indebted to Professor O. Augusto for the use of the oxygraph apparatus, and Professor E. Bechara for valuable discussions and suggestions. G.C. thanks CNPq and FAPESP (01/07309-0) for fellowships during her Ph.D. studies.

References

1. (a) S.K. Sridhar, S.N. Pandeya, J.P. Stables and A. Ramesh, *Eur. J. Pharm. Sci.*, **16**, 129 (2002); (b) A.E. Medvedev, A. Cow, M. Sandler and V. Glover, *Biochem. Pharmacol.*, **52**, 385 (1996); (c) V. Glover, A. Medvedev and M. Sadler, *Life Sci.*, **57**, 207 (1995).
2. (a) Y. Tozawa, A. Ueki, S. Manabe and K. Matsushima, *Biochem. Pharmacol.*, **56**, 1041 (1998); (b) J.E. Morley, S.A Farr and J.F. Flood, *Eur. J. Pharmacol.*, **305**, 23 (1996).
3. J.F.M. Silva, S.J. Garden and A.C. Pinto, *J. Braz. Chem. Soc.*, **12**, 273 (2001).
4. (a) S.E. Webber, J. Tikhe, S.T. Worland, S.A. Fuhrman, T.F. Hendrickson, D.A. Matthews, R.A. Love, A.K. Patick, J.W. Meador, R.A. Ferre, E.L. Brown, D.M. DeLisle, C.E. Ford and S.L. Binford, *J. Med. Chem.*, **39**, 5072 (1996); (b) M. Mohammadi, G. McMahon, L. Sun, C. Tang, P. Hirth, B.K. Yeh, S.R. Hubbard and J. Schlessinger, *Science*, **276**, 955 (1997).
5. S.N. Pandeya, D. Sriram, G. Nath and E. DeClercq, *Eur. J. Pharm. Sci.*, **9**, 25 (1999).
6. N. Karali, *Eur. J. Med. Chem.*, **37**, 909 (2002).
7. A. Cane, M.C. Tournaire, D. Barritault and M. Crumeyrolle-Arias, *Biochem. Biophys. Res. Commun.*, **276**, 379 (2000).
8. (a) C.V.R. Reddy and M.G.R. Reddy, *J. Chem. Eng. Data*, **39**, 723 (1994); (b) G.A. Bain, D.X. West, J. Krejci, J. Valdés-Martínez, S. Hernández-Ortega and R.A. Toscano, *Polyhedron*, **16**, 855 (1997); (c) V.I. Tsapkov, N. Al-Nabgali, V.V. Stan and N.M. Samus, *Russ. J. Gen. Chem.*, **64**, 1604 (1994).
9. (a) R.C. Khulbe, R.P. Singh and Y.K. Bhoon, *Transition Met. Chem.*, **8**, 59 (1983); (b) R.C. Khulbe, Y.K. Bhoon and R.P. Singh, *J. Indian Chem. Soc.*, **58**, 840 (1981).
10. D.X. West, A.K. El-Sawaf and G.A. Bain, *Transition Met. Chem.*, **23**, 1 (1998).
11. M.C. Rodríguez-Argüelles, A. Sanchez, M.B. Ferrari, G.G. Fava, C. Pelizzi, G. Pelosi, R. Albertini, P. Lunghi and S. Pinelli, *J. Inorg. Biochem.*, **73**, 7 (1999).
12. M.B. Ferrari, C. Pelizzi, G. Pelosi and M.C. Rodríguez-Argüelles, *Polyhedron*, **21**, 2593 (2002).
13. (a) A.M.A. Hassaan, *Transition Met. Chem.*, **15**, 283 (1990); (b) A.M.A. Hassaan, A.K.A. Al-Nasr and M.A. Khalifa, *J. Indian Chem. Soc.*, **74**, 496 (1997); (c) A.M.A. Hassaan, A.K.A. Al-Nasr and M.A. Khalifa, *Russ. J. Coord. Chem.*, **23**, 356 (1997).
14. A.M.A. Hassaan, *Syn. React. Inorg. Met. – Org. Chem.*, **27**, 835 (1997).
15. (a) S.P. Wolff, Z.Y. Jiang and J.V. Hunt, *Free Radical Biol. Med.*, **10**, 339 (1991); (b) S.P. Wolff and R.T. Dean, *Biochem. J.*, **245**, 243 (1987).
16. V.V. Mossine, M. Linetsky, G.V. Glinsky, B.J. Ortwerth and M.S. Feather, *Chem. Res. Toxicol.*, **12**, 230 (1999).
17. (a) R. Cheng and S. Kawakishi, *J. Agric. Food Chem.*, **42**, 700 (1994); (b) G.B. Sajithlal, P. Chithra and G. Chandrakasan, *Mol. Cell. Biochem.*, **194**, 257 (1999).
18. M.B. Yim, H.S. Yim, C. Lee, S.-O. Kang and P.B. Chock, *Ann. NY Acad. Sci.*, **928**, 48 (2001).
19. J.W. Eaton and M. Qian, *Mol. Cell. Biochem.*, **234/235**, 135 (2002).
20. R.T. Rodio, E.M. Pereira, M.M. Tavares and A.M.D.C. Ferreira, *Carbohydr. Res.*, **315**, 319 (1999).
21. G.R. Buettner and L.W. Oberley, *Biochem. Biophys. Res. Commun.*, **8**, 69 (1978).
22. (a) H. Kaur, *Free Rad. Res.*, **24**, 409 (1996); (b) H. Kaur, K.H.W. Leung and M.J. Perkins, *J. Chem. Soc., Chem. Commun.*, 142 (1981).

23. W.J. Geary, *Coord. Chem. Rev*., **7**, 81 (1971).
24. P. Guerriero, S. Tamburini and P.A. Vigato, *Coord. Chem. Rev*., **139**, 17 (1995).
25. D.R. Lide, (Ed.), *CRC Handbook of Chemistry and Physics*, 76th edit., Boca Raton, 1995/1996.
26. R.B. Cole, (Ed.), *Electrospray Ionization Mass Spectrometry*, Wiley, New York, 1997.
27. R. Colton, A. D'Agostinho and J.C. Traeger, *Mass Spectrom. Rev*., **14**, 79 (1995).
28. (a) J. Griep-Raming, S. Meyer, T. Bruhn and J.O. Metzger, *Angew. Chem. Int. Ed*., **41**, 2738 (2002); (b) R. Arakawa, S. Tachiyashiki and T. Matsuo, *Anal. Chem*., **67**, 4133 (1995); (c) E. Meurer, L.S. Santos, R.A Pilli and M.N. Eberlin, *Org. Lett*., **5**, 1391 (2003).
29. D.A. Plattner, *Int. J. Mass Spectrom*., **207**, 125 (2001).
30. E. Labisbal, A. Sousa, A. Castineiras, J.A. García-Vázquez, J. Romero and D.X. West, *Polyhedron*, **19**, 1255 (2000).
31. J. Muller, K. Felix, C. Maichle, E. Lengfelder and J. Strachle, *J. Inorg. Chim. Acta*, **233**, 11 (1995).
32. S.V. Singh, O.C. Saxena and M.P. Singh, *J. Am. Chem. Soc*., **92**, 537 (1970).
33. K.S. Rangappa, M.P. Raghavendra, D.S. Mahadevappa and D.C. Gowda, *Carbohydr. Res*., **307**, 253 (1998).
34. V.A. Yaylayan and A.A. Ismail, *Carbohydr. Res*., **276**, 253 (1995).
35. W.H. Koch and M.R. Cheedkel, *Biochim. Biophys. Acta*, **924**, 458 (1987).
36. C.A. Davies, B.R. Nielsen, G. Timmins, L. Hamilton, A. Brooker, R. Guo, M.C.R. Symons and P.G. Winyard, *Nitric Oxide: Biol. Chem*., **5**, 116 (2001).
37. (a) S. Oikawa and S. Kawanishi, *Biochemistry*, **35**, 4584 (1996); (b) T. Kocha, M. Yamaguchi, H. Ohtaki, T. Fukuda and T. Aoyagi, *Biochim. Biophys. Acta*, **1337**, 319 (1997).

TMCH 5896